11th International Workshop on Ship and Marine Hydrodynamics
Hamburg, Germany, September 22-25, 2019

A Modified Model for Waves Generated by a Moving Body in a Stratified Fluid with Free Surface

Y. Li[1, 2], K. Chen[1, 2, *], Y. You[1, 2]

[1]State Key Laboratory of Ocean Engineering, Shanghai Jiao Tong University, 200240 Shanghai, China
[2]Collaborative Innovation Center for Advanced Ship and Deep-Sea Exploration, 200240 Shanghai, China

*Corresponding author, raulphan@sjtu.edu.cn

ABSTRACT

The model proposed by Milder and further developed by Robey and You is capable of expressing the internal wave generated by a moving sphere or cylindrical body a satisfied fluid. Unfortunately, this model cannot describe the surface wave because of the rigid lid assumption. In this paper, a modified model is established with linearized governing equations and the free surface condition. This modified model can describe both the internal and surface wave excited by a submerged cylindrical body and is feasible to arbitrary density profiles. In the investigation, the eigenvalue parameter is obtained by solving the eigenvalue problem under the boundary condition through Thomson-Haskell method. The eigenvalue parameter is then employed to construct the Green function. The vertical displacement induced by the moving objects is obtained after solving the Green function through Fourier transform in finite or infinite water depth. The results are compared to experimental results and classical theory, respectively. The comparisons show good agreement. The results also show that the waveform consists of multiple wave modes from mode-0 to mode-*n*. It is also found that mode 0 is associated to the surface wave and the other modes are related to the internal waves.

1 INTRODUCTION

The fluid density commonly stratifies in the ocean due to the vertical distribution of temperature and salinity. Coupled with a certain source of excitation, e.g. a moving submerged body, surface wave and internal waves will be generated simultaneously. The study of surface waves began with Lord Kelvin[1], who for the first time proposed that the surface wave angle generated by a uniformly moving object is 19.47°. Compared with Kelvin waves, internal waves are more complex. Theoretical investigations of the internal wave patterns have been performed for a long time. According to the fundamental assumptions, theoretical models can be divided into two classes.

For the first class, the theories consider a multilayer fluid, and each layer has a uniform density. The two-layer model proposed by W. Yeung and T. C. Nguyen[2] is the most classical one in this class. They used the potential fluid theory by giving the Green function of point source in two layers of finite deep fluid upper layer and discussed the influence of surface waves mode and internal waves mode on the free surface and interface. By using the stationary phase method, they obtained the far-field asymptotic behaviour of surface waves and internal waves and found two different modes in surface waves and interface waves. Zhu Wei[3] further investigated the wave problem of three-dimensional objects in two-layer fluid, and established and solved the layered integral equation based on the four nodes isoparametric element method. The numerical results of free surface waves and internal waves are consistent with the theoretical model established by Yeung[2]. Based on Havelock[4]'s one-layer model, Timour[5] established the *n*-layer model excited by a mass force. The far-field asymptotical solutions of the waves were given. The research found that for each mode divergent and transverse are present if the speed of the object is less than the critical velocity U_i, and only the divergent component is sustained in the supercritical regime, but the solution of the interfaces below the

moving object can't be obtained. However, this class of theories assumes that the density is constant in each layer, resulting infinite Brunt–Vaisala frequency at the interface of the neighbouring layer and zero frequency in each layer, which is far from the practical situation.

The theories of the second class have better treatment on density distribution. These theories also consider a multilayer fluid, but each layer has a linear density change, so that the Brunt–Vaisala frequency can be easily obtained. The first model in this class is the two-dimensional Lee wave model proposed by Long[6, 7]. Miropolsky[8] and Sekerzh-zenkovich[9] further developed the three-dimensional Lee wave model. The internal wave problem of a point source in an infinite stratified fluid was systematically analysed by Voisin[10, 11]. Because the source and sink cannot reflect the disturbance of real objects, many scholars have studied the theory of internal wave induced by mass sources. Milder[12] established an equivalent mass source consisted of a series of sources and sinks with a uniform translational speed. Robey[13] then proposed the cylinder-shaped mass source model, and verified this method using the experimental results. You[14] designed a spheroid-shaped source model based on Robey's work and has a better result.

Unfortunately, the theoretical model in the second class taking the rigid lid assumption in their derivation. Under such a condition, the free surface wave is eliminated and the waves near the free surface are suppressed. In this paper, a modified model is derived considering the free surface condition instead of the rigid lid surface condition. The problem of a uniform motion object generating surface waves in a stable layered fluid with finite or infinite depth was discussed. The model was verified by using experimental results of internal wave and classical theory of surface wave. The characteristics of different modes are further analysed.

2 THEORETICAL METHOD

Here we consider the dynamics of small-amplitude periodic internal waves generated by a moving source with constant velocity U in a stratified. Fig 1. plots the definition of system. The cartesian coordinates are established with x (track), y (cross-track), and z (depth, positive downward). The x coordinate in the moving coordinate system with source is $\bar{x}$ that can be expressed as $\bar{x} = x - Ut$. In the moving coordinate the y and z coordinate don't change with time. With the assumptions, the linearized governing equations reduce to:

$$\begin{cases} \bar{\rho}\dfrac{\partial u}{\partial t} = -\dfrac{\partial p}{\partial x} \\ \bar{\rho}\dfrac{\partial v}{\partial t} = -\dfrac{\partial p}{\partial y} \\ \bar{\rho}\dfrac{\partial w}{\partial t} = -\dfrac{\partial p}{\partial z} - \rho g \\ \dfrac{\partial u}{\partial x} + \dfrac{\partial v}{\partial y} + \dfrac{\partial w}{\partial z} = Q(\mathbf{x},t) \\ \dfrac{\partial \rho}{\partial t} + w\bar{\rho}' = 0 \end{cases} \tag{1}$$

where $\bar{\rho}(z)$ is the background density profile, which is only a function of z, and ρ is the fluctuation density. $Q(\mathbf{x},t)$ is the volume flow rate of the equivalent mass source and can be expressed as $Q = \int_{-a}^{a} q(\xi)\delta(\bar{x} - \xi)d\xi\delta(y)\delta(z - z_0)$. $q(\xi) = UdS / d\xi$ is the volume flow rate at $x = Ut + \xi$, and $S(\xi)$ is the sectional area at $x = Ut + \xi$. The $q(\xi)$ can regarded as source intensity.

Apply the Eq. 1 to eliminate the disturbance pressure p, disturbance density ρ and velocity components u, v in the equation, the governing equation of vertical velocity w can write as:

$$\frac{\partial^2}{\partial t^2}[\frac{\partial}{\partial z}(\bar{\rho}\frac{\partial w}{\partial z}) + \bar{\rho}\nabla_h^2 w] + \bar{\rho}N^2\nabla_h^2 w = \frac{\partial^3}{\partial t^3 \partial z}(\bar{\rho}Q) \tag{2}$$

where the Brunt–Vaisala frequency N defines as $N^2 = g / \bar{\rho} \cdot \partial\rho / \partial z$, and the Laplace operator in the horizontal defines as $\nabla^2 \equiv \dfrac{\partial^2}{\partial x^2} + \dfrac{\partial^2}{\partial y^2}$.

In this paper, the Boussinesq approximation is not considered. The dispersion relationship of internal wave without Boussinesq approximation has been discussed by Cai [16].

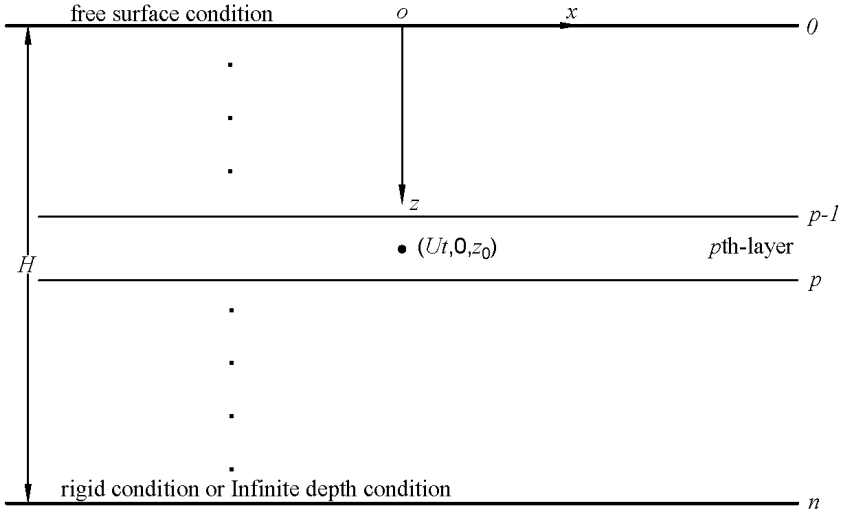

Fig.1. Definition of coordinate system

For the boundary conditions, we will introduce two boundary conditions (the fluid with free surface in infinite depth or finite depth). For the linearized boundary conditions of the free surface, the relationships are:

$$\frac{dp}{dt}=0,\ w=\frac{d\zeta}{dt},\quad \text{for } z=0 \tag{3}$$

The linear free surface boundary condition can be obtained by eliminating the disturbance pressure p with Eq. 1 and 3:

$$\frac{\partial^3(w)}{\partial t^2\partial z}=g\nabla_h^2 w,\ \ z=0 \tag{4}$$

Consider a flat bottom, there is $w=0$ in $z=H$ for finite depth. For the infinite depth, the solution of vertical velocity for $z>H$ is proportional to e^{-kz}, so there is $w'=kw$ in $z=H$ The bottom condition can be written as:

$$\begin{cases} w=0 \ for\ z=H \ \text{(finite depth)} \\ w'=kw \ for\ z=H \ \text{(infinite depth)} \end{cases} \tag{5}$$

The relationship between vertical displacement with vertical velocity is $w=d\eta/dt$. Substitute this relationship into Eq.2, 4, 5 and apply the Fourier transform in the horizontal direction. The governing equations become:

$$(\overline{\rho}\overline{\eta}')'+k^2\overline{\rho}(\frac{N^2}{\omega^2}-1)\overline{\eta}=\overline{Q}(\overline{\rho}\delta(z-z_0))' \tag{6}$$

$$\omega^2\overline{\eta}'=gk^2\overline{\eta},\ \ z=0 \tag{7}$$

$$\begin{cases} \overline{\eta}=0,\ z=H \ \text{(finite depth)} \\ \overline{\eta}'=k\overline{\eta}\ ,\ z=H \text{(infinite depth)} \end{cases} \tag{8}$$

$\overline{\eta}(k_x,k_y,z)$ stands for the two-dimensional Fourier transform of the corresponding variable $(\overline{x},y)$ and $\overline{Q}=-iU/\omega\int_{-a}^{a}q(\xi)e^{i\omega\xi/U}d\xi$; k stands for horizontal wave number, $k^2=k_x^2+k_y^2$, where k_x and k_y. To solve this equation, we must first solve the corresponding eigen equations and obtain its eigen function.

$$(\overline{\rho}\phi')'+k^2\overline{\rho}(\frac{N^2}{\omega^2}-1)\phi=0 \tag{9}$$

$$\omega^2\frac{\partial\phi}{\partial z}=gk^2\phi,\ \ z=0 \tag{10}$$

$$\begin{cases} \phi=0,\ z=H \ \text{(finite depth)} \\ \phi'=k\phi,\ z=H \ \text{(infinite depth)} \end{cases} \tag{11}$$

The solution of this problems is based on Thomson-Haskell method[15] without Boussinesq approximation and rigid lid assumption. The stratified fluid should be vertically divided into *n* layers, and in each layer the Brunt–Vaisala frequency *N* is constant, which means the density has a linear distribution in

each layer. At the *p*th layer, the label of the upper interface is recorded as *p*-1, and the label of the lower interface is recorded as *p* as show in Fig. 1. Then its original Eq.9 becomes:

$$\phi_p(z)'' + N_p^2\phi_p'(z)/g + k^2\overline{\rho}(\frac{N_p^2}{\omega^2}-1)\phi_p(z) = 0 \tag{12}$$

Its general solution is:

$$\phi_p(z) = e^{-\varepsilon z}(A_p e^{\lambda_p z} + B_p e^{-\lambda_p z}) \tag{13}$$

where $\varepsilon = N_p^2/(2g)$, $\lambda_p = (m_p^2-\varepsilon^2)^{1/2}$, $m_p = k[(N_p^2-\omega^2)/\omega^2]^{1/2}$.

Through some mathematical operations, the following relationships can be obtained:

$$(\dot{\phi}_p, \phi_p) = \frac{e^{-\varepsilon h_p}}{\lambda_p}\begin{bmatrix} -\varepsilon\sin(\lambda_p h_p)+\lambda_j\cos(\lambda_p h_p) & -\sin(\lambda_p h_p) \\ (\lambda_p^2+\varepsilon^2)\sin(\lambda_p h_p) & \varepsilon\sin(\lambda_p h_p)+\lambda_j\cos(\lambda_p h_p)\end{bmatrix}(\dot{\phi}_{p-1}, \phi_{p-1})^T \tag{14}$$

where h_p is the thickness of the *p*th layer of fluid. Through the multiplication operation, finally, the relationship between the 0th interface and the nth interface is obtained.

$$(\dot{\phi}_n, \phi_n) = F(\dot{\phi}_0, \phi_0)^T \tag{15}$$

where $F = \begin{bmatrix} F_{11} & F_{12} \\ F_{21} & F_{22}\end{bmatrix} = a_n a_{n-1}\cdots a_2 a_1$, $a_p = \frac{e^{-\varepsilon h_p}}{\lambda_p}\begin{bmatrix} -\varepsilon\sin(\lambda_p h_p)+\lambda_p\cos(\lambda_p h_p) & -\sin(\lambda_p h_p) \\ (\lambda_p^2+\varepsilon^2)\sin(\lambda_p h_p) & \varepsilon\sin(\lambda_p h_p)+\lambda_p\cos(\lambda_p h_p)\end{bmatrix}$.

Then substitute the boundary condition into this equation, taking the infinite water depth as an example:

$$\begin{cases} \phi_n = F_{11}\dfrac{gk^2}{\omega^2}\phi_0 + F_{12}\phi_0 \\ \phi_n/k = F_{21}\dfrac{gk^2}{\omega^2}\phi_0 + F_{22}\phi_0 \end{cases} \tag{16}$$

Eliminate the ϕ_0, ϕ_n to get the solution of this transcendental equation:

$$k(F_{21}\frac{gk^2}{\omega^2}+F_{22}) - (F_{11}\frac{gk^2}{\omega^2}+F_{12}) = 0 \tag{17}$$

For a given *k* value, the dispersion relation is obtained by solving the nonlinear Eq.17. There are many methods to solve the equation, the most commonly used method is the iterative method. It is worth noting that for each *k* there are countless solutions, so there are countless ω_m corresponding to it, each discrete value corresponds to a mode.

Therefore, for this eigen problem, each *k* corresponds to different eigen values $\omega_m(k)$. The corresponding internal wave phase velocity and wave group velocity can be expressed as:

$$c_{pm} = \frac{\omega_m(k)}{k}, \quad c_{gm} = \frac{d\omega_m(k)}{dk} \tag{18}$$

With free surface condition, this problem becomes a regular Sturm-Liouville problem with eigenvalue parameter in the boundary condition, which was investigated by Walter[17] and Fulton[18]. By structuring the Hilbert space $H = L^2[0,\pi]\oplus C$, the asymptotic solution of the eigen functions are given and the problem of eigen function expansion has been discussed. Some of the most useful conclusions in Fulton's article are listed below. For a function in space $F = \begin{pmatrix} F_1(x) \\ F_2\end{pmatrix}$, $G = \begin{pmatrix} G_1(x) \\ G_2\end{pmatrix}$, $H = L^2[0,\pi]\oplus C$ the inner product in space is defined as:

$$(F,G) = \int_a^b F_1(x)\overline{G_1(x)}dx + \frac{1}{\alpha}F_2G_2 \tag{19}$$

where α, F_2, G_2, are given by the boundary conditions, for our problems $\alpha = g$, $F_2 = gF_1(0)$, $G_2 = gG_1(0)$. For the eigen function Φ_n of this problem, its orthogonality is:

$$(\Phi_n, \Phi_m) = 0, \quad \mathrm{m} \neq \mathrm{n} \tag{20}$$

Therefore, the orthonormal basis for the eigen function is:

$$\Psi_n = \frac{\Phi_n}{\|\Phi_n\|} \tag{21}$$

With mean square convergence at $[a,b]$ for any $F_1 \in L_2[a,b]$, it can be expanded by the standard orthogonal basis:

$$F_1(x)=\sum_{n=0}^{\infty}(\int_a^b F_1\Psi_n dx)\Psi_n \tag{22}$$

The ϕ_p value of each layer can be calculated by the multiplication calculation. Then the eigen function can easily obtain by moving the origin of reference coordinate system to the upper bound of each layer.

$$\begin{cases}\phi_p(z)=e^{\varepsilon z}[C_p\cos(\lambda_j z)+D_p\sin(\lambda_j z)]\\ \dot{\phi}_p(z)=e^{\varepsilon z}[E_p\cos(\lambda_j z)+F_p\sin(\lambda_j z)]\end{cases}\ (0<z<h_p) \tag{23}$$

where $C_p=\phi_{p-1}$, $D_p=-\dfrac{(\varepsilon_p\phi_{p-1}+\dot{\phi}_{p-1})}{\lambda_p}$, $E_p=\dot{\phi}_{p-1}$, $F_p=[(\lambda_p+\dfrac{\varepsilon_p^2}{\lambda_p})\phi_{p-1}+\dfrac{\varepsilon_p\dot{\phi}_{p-1}}{\lambda_p}]$.

Through formula Eq.21, the orthonormal basis Ψ_n can be obtained.

After analysing the eigen problems corresponding to equations Eq. 9, 10 and 11, the Green function method can be used to solve the problem:

$$\frac{\partial^2 G}{\partial z^2}+k^2(\frac{N^2}{\omega^2}-1)G=\delta(z-z_0) \tag{24}$$

$$\omega^2\frac{\partial G}{\partial z}=gk^2G,\ \ z=0;G=0,\ z=H \tag{25}$$

The corresponding Green function can be obtained by using Eq. 22:

$$G(z;z_0)=-\frac{1}{k^2}\sum_{m=1}^{+\infty}\frac{\omega^2\omega_m^2}{\omega^2-\omega_m^2}\Psi_m(z)\Psi_m(z_0) \tag{26}$$

So the solution of $\bar{\eta}$ is：

$$\bar{\eta}(k_x,k_y,z)=\frac{\bar{\rho}}{k^2}\sum_{m=1}^{+\infty}\frac{\bar{Q}\omega^2\omega_m^2}{\omega^2-\omega_m^2}\Psi_m(z)\Psi_m'(z_0) \tag{27}$$

By taking the inverse Fourier transform of k_x, the solution of $\tilde{\eta}(\bar{x},k_y,z)$ can be obtained：

$$\tilde{\eta}(\bar{x},k_y,z)=\frac{i\bar{\rho}}{2U}\sum_{m=1}^{+\infty}\frac{\bar{Q}(\omega_m)c_{\mathrm{p}m}^{\ 3}k}{1-c_{\mathrm{p}m}c_{\mathrm{g}m}/U^2}\Psi_m(z)\Psi_m'(z_0)e^{-i\omega_m\bar{x}/U} \tag{28}$$

Then the vertical displacement of the moving mass source can be obtained by using IFFT.

For ellipse-shaped mass source with long and short axes 2*a* and 2*b* respectively, the corresponding cross-sectional area is $S(\xi)=\begin{cases}\pi b^2(1-\xi^2/a^2),\ (|\xi|\le a)\\ 0,\ (|\xi|>a)\end{cases}$. The vertical displacement corresponding to the equivalent ellipse-shaped mass source can be written as:

$$\tilde{\eta}(\bar{x},k_y,z)=\frac{2\pi b^2 ai\bar{\rho}}{U}\sum_{m=1}^{+\infty}\frac{\sin(\omega_m a/U_s)/(\omega_m a/U_s)-\cos(\omega_m a/U_s)}{(\omega_m a/U_s)^2}\times\frac{c_{\mathrm{p}m}^{\ 3}k}{1-c_{\mathrm{p}m}c_{\mathrm{g}m}/U^2}\Psi_m(z)\Psi_m'(z_0)e^{-i\omega_m\bar{x}/U} \tag{29}$$

3 COMPARSION AND DISSCUSION

3.1 Comparison with experiments

Internal wave has been investigated by many scholars both in theory and experiment. In recent year, Wang[19] experimentally investigates the behaviour of wave height and wave pattern. In his work, four different towing models are used with the diameter of 0.07m and the aspect ratio of 1, 4, 7, 9. In this paper we choose the models with the aspect ratio of 7 for comparison. In the study, different velocity amplitudes are obtained by calculating based on the equation Eq.29. The quantitative comparison of wave height is shown in Fig.2. The maximum peak-to-peak displacement variation of internal waves is regarded as the wave height *H*. The dimensionless wave height H/D is plotted in Fig. 2 versus the towing velocity *U*. The asterisk sign represents the experimental data. The black line represents the result of numerical calculations. The amplitude first increases and then decreases as the speed increases. The amplitude reaches its peak at speed 15cm/s which slightly lower than the critical velocity of internal wave modal propagation which nearly equal to 19cm/s. Generally, numerical simulation results agree to the experimental results.

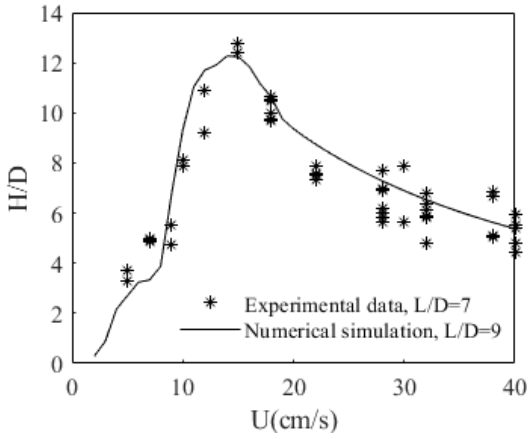

Fig.2. Experimental and numerical internal wave height *H/D* vs towing speed *U*

3.2 Comparison with classical theory

We choose the one-layer model to compare the characteristics of the surface wave because of the lack of experiments. For Havelock's one-layer theory, the surface displacement generated by a pressure field $p(x,y)$ moving in the *x* direction with constant speed *U* have far-field asymptotic solution[20]:

$$Z(x,y) \simeq i\pi \int_{-\pi/2}^{\pi/2} d\theta \frac{\hat{P}(K_0(\theta),\theta)\exp[-i(\cos\theta X - \sin\theta Y)/(Fr^2\cos^2\theta)]}{Fr^4\cos^4\theta} \tag{30}$$

where *X*, *Y*, *Z*, *K*, $\hat{P}$ are non-dimensional parameters. For the typical size *b*, these parameters have the relationships:

$$Z = \frac{4\pi^2\zeta}{b},\ X = \frac{x}{b},\ Y = \frac{y}{b},\ K = kb,\ \hat{P} = \frac{\hat{p}}{\rho g b^3} \tag{31}$$

The pressure point is given by a Gaussian pressure field of typical size *b*, symmetrical around the origin. For the comparison, we consider a small ball with a diameter of *b* at an infinite water depth with no density change. The behaviour of the ball and pressure point is similar. However, it is impossible to give no density changed profile for our method. Consider a linear variation density profile with a density gradient of $0.01kg/m^4$. Then the surface wave displacement field generated by a small ball can be obtained by using the modified model in different Froude number. Fig. 3 shows a typical Kelvin wave system by the proposed method. Fig. 4 shows the results of mode-0 calculated by Eq.30. Comparing the two figures, they show similar characteristics of waveform as *Fr* increases.

Alexandre[20] found that the maximum amplitude of the surface wave was proportional to Fr^{-1} at a high Froude number. The maximum amplitude corresponds to an angle calculated by interpolating the maxima of the wave amplitudes over one wavelength sufficiently far from the perturbation. Fig. 5 shows the relationship between angular of maximum amplitude of the surface wave with Froude number. The horizontal axis shows the Froude number, and the vertical axis shows the angular of maximum amplitude of the surface wave. In Fig.5, the dashed black line represents the Kelvin angle $\phi_k = \arcsin(1/3)$. The black full line is a straight line which is inversely proportional to the Fr to fit the change of angular in large Fr.

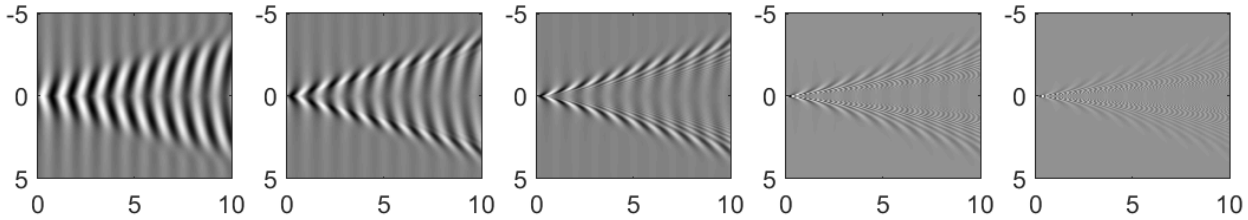

(a)*Fr*=0.3 (b)*Fr*=0.5 (c)*Fr*=1 (d)*Fr*=2 (e)*Fr*=3

Fig.3. Surface displacement computed using modified model for different Froude numbers

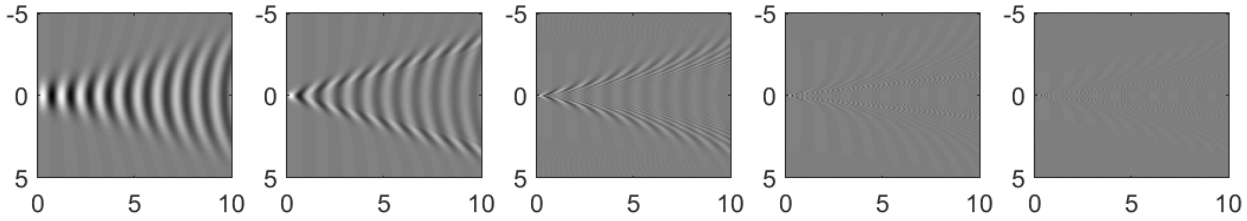

(a)*Fr*=0.3 (b)*Fr*=0.5 (c)*Fr*=1 (d)*Fr*=2 (e)*Fr*=3

Fig.4. Surface displacement generated by a pressure point for different Froude numbers

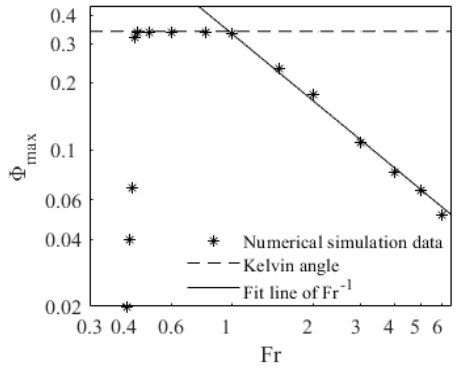

Fig.5. Angular of maximum amplitude of the surface wave vs Froude number

The similar wave characteristics of mode-0 and the classical theory reveals that the adoption of free surface condition enables the modified model to express the surface wave. Although the precision is not clear yet, the modified model at least can provide satisfying result when the problem degenerates to one-layer.

3.3 Discuss the characterize of the different modes

The modal dispersion relation and eigen function are of great importance on affecting the displacement field. For further discussion, one case was chosen to present the wave behaviours of different mode. Consider a typical fluid environment, including an upper layer and a lower layer with a constant density ρ_1 and ρ_2, respectively, and a mixing layer between the two layers. The mixing layer, also termed as pycnocline, is designed to have a smooth density profile obeying the sigmoid function:

$$\rho(z) = (\rho_2 - \rho_1) / (1 + e^{-16z/\Delta}) + \rho_1 \tag{32}$$

where Δ is the thickness of the mixing layer. The upper fluid and lower fluid depth are h_1 and h_2. In this case, $\rho_1 / \rho_2 = 0.97$, $h_1 = h_2 = \Delta = 10m$.

Fig.6 shows the variation of the wave frequency, phase velocity and group velocity versus the wave number in the first three modes. As shown in Fig.6, when the wave number *k* increases, the internal wave frequency has a monotonic increase while the phase and group velocity both have a monotonic decrease. It should be noted that frequency and the velocities are obviously larger for the mode-0.

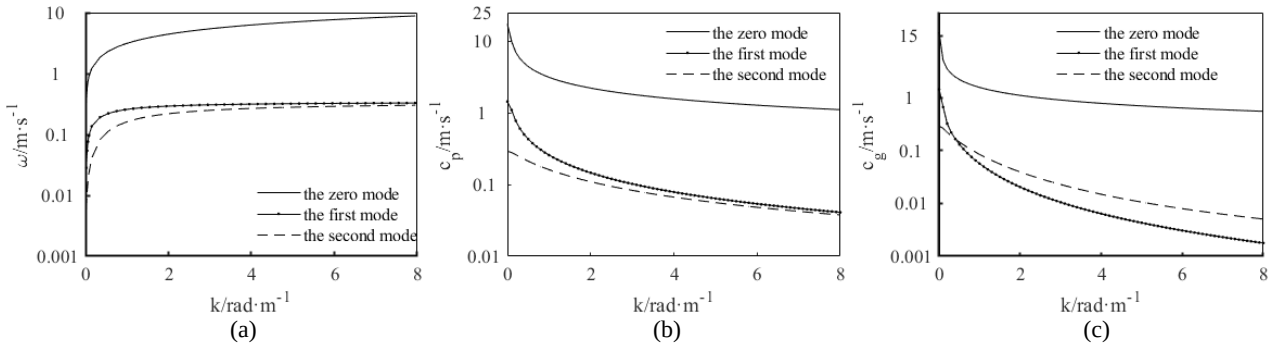

(a) (b) (c)

Fig.6. The variation of the wave frequency, phase velocity and group velocity versus the wave number for the first three modes:
(a) Dispersion relation (b) phase velocity vs. wave number (c) group velocity vs. wave number

Fig.7 shows vertical distribution of eigen function in the first three modes. In each mode, the eigen function corresponding to three different wave numbers are given by different line type. The eigen function of mode-*m* corresponds to *m* peaks vertically. The vertical eigen function of the mode-0 begins to decay directly from the surface. For the internal wave mode, it reduces gradually along both sides. The greater the wave number, the faster the eigen function value attenuates.

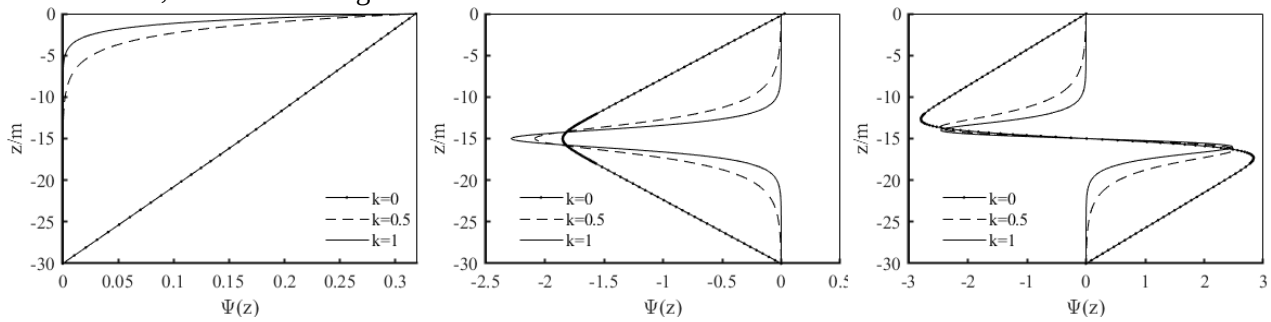

(a) (b) (c)

Fig.7. Normalized vertical feature function in the first three modes

(a) the mode-0 (b) the mode-1 (c) the mode-2

Fig.8 shows the vertical distribution of the eigen function derivative in the first three modes. Similarly, three different wave numbers are given by different line type. For the mode-0, the derivative of eigen function have a montonic decrease from surface. As *k* decreases, the decay rate of eigen function generally reduces. Especially the decay rate goes down to zero when *k*=0. For the rest modes, the eigen function derivative has *m*+1 peaks for mode-*m*. The value of the eigen function derivative also decreases along both sides.

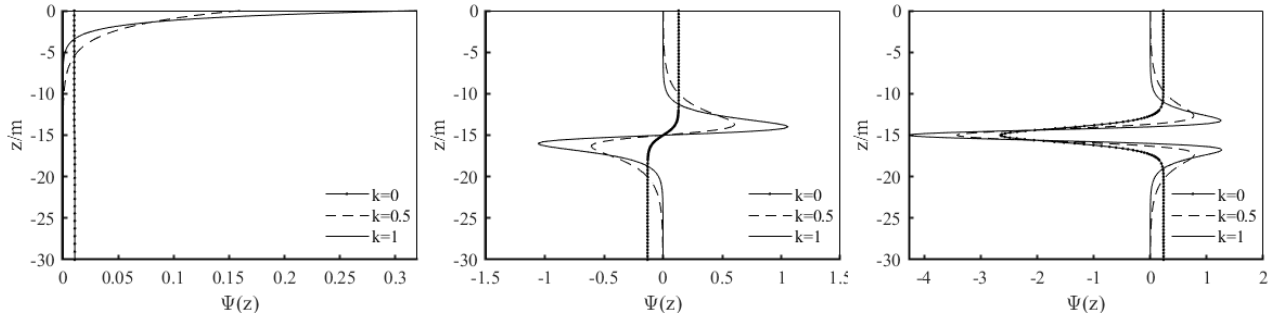

(a) (b) (c)

Fig.8. The derivative of normalized vertical feature function in the first three modes

(a) the mode-0 (b) the mode-1 (c) the mode-2

It is noticed that eigen function directly affect the amplitude of wave based on Eq. 29. In this equation, z represents the location of displacement field and z_0 represents the location of the mass source. Thus, the vertical distribution of the eigen function actually reveals the amplitude distribution of the corresponding wave mode. Meanwhile, the value of eigen function derivative demonstrates the magnitude of the disturbance induced by the mass source at the corresponding location. According to the analysis above, the mode-0 waves have the maximum amplitude at the surface. When the waves spread to deeper fluid, the amplitudes decline quickly, and the wave of larger wave number shows the greater decline speed. For the internal waves, the maximum amplitudes occur in the pycnocline and are located at different position for different mode. If the mass source is outside the pycnocline, the internal waves amplitude will be larger when the source becomes closer to the pycnocline. If the mass source is inside the pycnocline, the internal waves amplitude of each mode will be larger when the source is closer to the position that is associated to eigen function derivative peaks.

4 SUMMARY

In this paper, a modified model is derived from Milder's theory with free surface condition. Eigen function, which can be regard as a regular Sturm-Liouville problem with eigenvalue parameter in the boundary condition, is solved by the Thomson-Haskell method[15] without Boussinesq approximation. Based

on the Green function method, the solution of the vertical displacement is finally derived. Some comparisons with experiment and one-layer theory are performed to support the modified model.

The solution shows that the waves consist of countless modes. Some characteristics of different modes are further discussed. There is a significant difference between the mode-0 and other modes. According to the mode properties, it can be divided into surface wave modes (the mode-0) and internal wave modes (other modes). The eigen function of the mode-*m* has m peaks in the *z* direction, and the derivative of the eigen function of the internal wave mode has (*m*+1) peaks vertically. The wave amplitude distribution of each wave mode can be estimated by the vertical distribution of the eigen function. The magnitude of the disturbance of the mass source can be estimated by the eigen function derivative.

ACKNOWLEDGEMENTS

We gratefully acknowledge financial support from the National Natural Science Foundation of China (Grant No.11802176).

REFERENCES

[1] Thomson W. On ship waves[J]. Proceedings of the Institution of Mechanical Engineers, 1887,38(1):409-434.
[2] Yeung R W, Nguyen T C. Waves Generated by a Moving Source in a Two-Layer Ocean of Finite Depth[J]. Journal of Engineering Mathematics, 1999,35(1):85-107.
[3] Zhu W, You Y, Miao G, et al. Waves generated by a 3 D moving body in a two-layer fluid of finite depth.[J]. Journal of Hydrodynamics, Series B, 2005,17(1):92-101.
[4] Havelock T H. The propagation of groups of waves in dispersive media, with application to waves on water produced by a travelling disturbance[J]. Proceedings of the Royal Society of London. Series A, Containing Papers of a Mathematical and Physical Character, 1908,81(549):398-430.
[5] Radko T. Ship Waves in a Stratified Fluid[J]. Journal of Ship Research, 2001,45(1):1-12.
[6] Long R R. Some Aspects of the Flow of Stratified Fluids: I. A Theoretical Investigation[J]. Tellus, 1953,5(1):42-58.
[7] Long R R. Some aspects of the flow of stratified fluids: II. Experiments with a two - fluid system[J]. Tellus, 1954,6(2):97-115.
[8] Miropol'Skii Y Z. Self-similar solutions of the Cauchy problem for internal waves in an unbounded fluid[J]. Izv. Akad. Nauk SSSR, Fizika Atmos. Okeana, 1978,14.
[9] Sekerzh-Zen'Kovich S Y. A fundamental solution of the internal-wave operator, 1979[C].1979.
[10] Voisin B. Internal wave generation in uniformly stratified fluids. Part 1. Green's function and point sources[J]. Journal of Fluid Mechanics, 1991,231:439-480.
[11] Voisin B. Internal wave generation in uniformly stratified fluids. Part 2. Moving point sources[J]. Journal of Fluid Mechanics, 1994,261(1):333-374.
[12] Milder M. Internal Waves Radiated by a Moving Source. Volume 1. Analytic Simulation[J]. 1974.
[13] Robey H F. The generation of internal waves by a towed sphere and its wake in a thermocline[J]. Physics of Fluids, 1997,9(11):3353-3367.
[14] You Y, Zhao X, Chen K, et al. An equivalent mass source method for internal waves generated by a body moving in a stratified fluid of finite depth[J]. 2009.
[15] Fliegel M, Hunkins K. Internal wave dispersion calculated using the Thomson-Haskell method[J]. Journal of Physical Oceanography, 1975,5(3):541-548.
[16] Cai S, Gao Z. A Numerical Method of Internal Waves Dispersion Relation., 1995[C].1995.
[17] Walter J. Regular eigenvalue problems with eigenvalue parameter in the boundary condition[J]. Mathematische Zeitschrift, 1973,133(4):301-312.
[18] Fulton C T. Two-point boundary value problems with eigenvalue parameter contained in the boundary conditions[J]. Proceedings of the Royal Society of Edinburgh: Section A Mathematics, 1977,77(3-4):293-308.
[19] Wang H, Chen K, You Y. An investigation on internal waves generated by towed models under a strong halocline[J]. Physics of Fluids, 2017,29(6):65104.
[20] Darmon A, Benzaquen M, Raphaël E. Kelvin wake pattern at large Froude numbers[J]. Journal of Fluid Mechanics, 2014,738.